Thin Solid Films 642 (2017) 157–162

Contents lists available at ScienceDirect

Thin Solid Films

journal homepage: www.elsevier.com/locate/tsf

Thickness-dependent thermal properties of amorphous insulating thin films measured by photoreflectance microscopy

A. Al Mohtar[a,b], G. Tessier[a,*], R. Ritasalo[c], M. Matvejeff[c], J. Stormonth-Darling[d], P.S. Dobson[e], P.O. Chapuis[f], S. Gomès[f], J.P. Roger[b]

[a] Laboratoire de Neurophotonique UMR8250, CNRS, Faculté des sciences biomédicales et fondamentales, Université Paris Descartes, 75270 Paris, France
[b] ESPCI Paris, PSL Research University, CNRS, Institut Langevin, 1 rue Jussieu, 75005 Paris, France
[c] Picosun Oy, Tietotie 3, 02150 Espoo, Finland
[d] Kelvin Nanotechnology Ltd, Rankine Building, Oakeld Ave, Glasgow G12 8LT, UK
[e] Electronics & Nanoscale Engineering, School of Engineering, University of Glasgow, G12 8QQ, UK
[f] Univ Lyon, CNRS, INSA-Lyon, Université Claude Bernard Lyon 1, CETHIL UMR5008, F-69621 Villeurbanne, France

ARTICLE INFO

Keywords:
Thermal conductivity
Thermal diffusivity
Interfacial thermal resistance
Frequency-domain photoreflectance
Atomic layer deposition

ABSTRACT

In this work, we report on the measurement of the thermal conductivity of thin insulating films of SiO_2 obtained by thermal oxidation, and Al_2O_3 grown by atomic layer deposition (ALD), both on Si wafers. We used photoreflectance microscopy to determine the thermal properties of the films as a function of thickness in the 2 nm to 1000 nm range. The effective thermal conductivity of the Al_2O_3 layer is shown to decrease with thickness down to 70% for the thinnest layers. The data were analyzed upon considering that the change in the effective thermal conductivity corresponds to an intrinsic thermal conductivity associated to an additional interfacial thermal resistance. The intrinsic conductivity and interfacial thermal resistance of SiO_2 were found to be equal to 0.95 W/m·K and 5.1×10^{-9} m^2K/W respectively; those of Al_2O_3 were found to be 1.56 W/m·K and 4.3×10^{-9} m^2K/W.

1. Introduction

Thermal and electronic conductivities are strongly correlated in most materials. However, many applications demand the maximization of one of these properties while minimizing the other. In microelectronics for instance, good electrical insulation is essential (capacitors, interconnects), but low-k dielectrics usually come with poor thermal conductivity, hampering heat dissipation. Conversely, high electrical conductivity and thermal insulation are crucial for thermoelectric conversion, in order to avoid Joule heating while preserving the temperature gradient [1,2]. Nanostructured materials offer a new way to act on these antagonistic requirements, since nanoscale thermal properties can significantly differ from bulk values [3,4]. A lot of attention has been focused recently on understanding the underlying physics, like phonon scattering [5] and heat transport phenomena [6,7].

In this paper, we investigate the thermal properties of two electrical insulators, SiO_2 and Al_2O_3 thin films. SiO_2 is essential to microelectronics and other industrial applications. It has therefore received a lot of attention, and its thermal properties are relatively well known. Some research groups have studied the thermal conductivity of Al_2O_3 amorphous thin films [8–11], but the evaluation of their interfacial thermal resistances is still very incomplete [12]. Al_2O_3 amorphous thin films are promising, since they can reduce electronic recombination losses in solar cells by the passivation of silicon surfaces, thus enabling higher efficiency [13]. Moreover, thin amorphous Al_2O_3 films are good thermal insulators as well as excellent moisture barriers [14] that can be fabricated at low temperatures [15,16], making them highly desirable in electronic components [17].

A broad range of experimental methods is available in order to determine the thermal properties of materials. They essentially differ in their heat generation process (optical, Joule, …), in the property which is probed (temperature of the surface, sample or air, acoustic waves, etc.…), and in the probing mechanism (refractive index, thermal emission, interferometry, fluorescence, electrical resistance…). Temporally, various strategies have also been developed: steady state, transient or modulated. Several reviews of thin films characterization techniques have been proposed [18,19]. Among these techniques, modulated photoreflectance microscopy has the advantages of being contactless, non-destructive and, owing to the high spatial resolution of visible light microscopy, allows measurements on relatively small samples (> 10 μm). It is based on the generation of thermal "waves" by intensity-modulated optical excitation. This technique was first

* Corresponding author.
E-mail address: gilles.tessier@parisdescartes.fr (G. Tessier).

http://dx.doi.org/10.1016/j.tsf.2017.09.037
Received 16 February 2017; Received in revised form 7 September 2017; Accepted 17 September 2017
Available online 19 September 2017

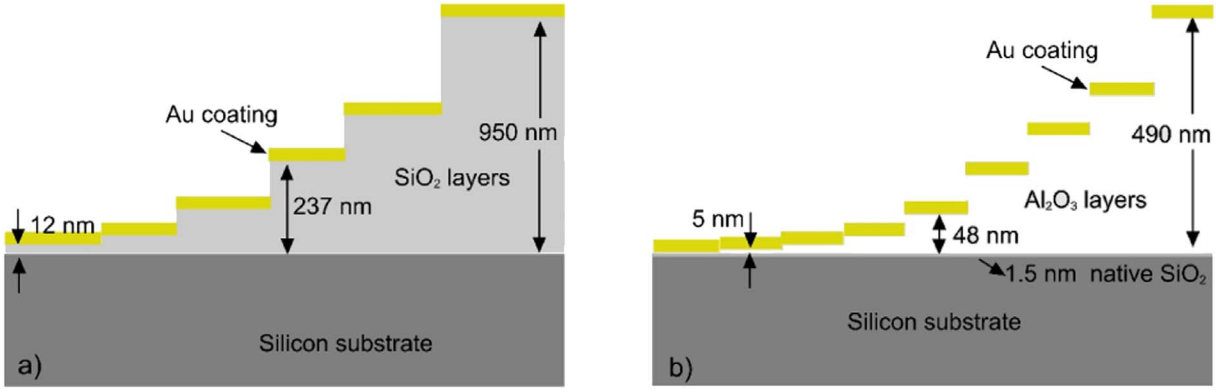

Fig. 1. Schematic of the fabricated samples, a) the SiO_2 layers and b) the Al_2O_3 layers.

proposed by A. Rosencwaig et al. [20], and then widely used to determine the thermal properties of bulk materials [21,22], grains [23], coatings and thin films [24,25]. In this work, the frequency domain photoreflectance method is used to study the effect of thickness on the thermal properties of amorphous SiO_2 and Al_2O_3 thin films. The method requires the deposition of a gold layer to opacify the surface, but is well adapted to this kind of study, where different nanoscale layers have to be distinguished. A 3D heat diffusion model was used to extract the thermal properties of each material independently [22].

2. Experimental

The SiO_2 thin films with different thicknesses were fabricated by Kelvin Nanotechnology Ltd. (KNT), in collaboration with Glasgow University. The starting material is a thick layer of SiO_2 grown by thermal oxidation on a p-type Si wafer. Repeated photolithography steps, followed by timed hydrofluoric acid (HF) etching, were performed to obtain the required thicknesses of 12, 30, 65, 145, 237, 530 and 950 nm, as depicted in Fig. 1a). The layer thickness was measured by white light interferometry [26].

The studied Al_2O_3 samples were fabricated by Picosun using a Picosun™ ALD reactor. ALD is a powerful method to grow fully conformal, pinhole-free layers with atomic accuracy [27]. This is based on the self-terminating nature of gas-solid reactions taking place at the sample surface. The studied thin films were grown on silicon wafer with a 10–14 μm n-type epilayer of resistivity 3–6 Ω·cm and a native SiO_2 layer (thickness of approximately 1.5 nm). The values of the obtained thicknesses (2, 5, 9.5, 24, 48, 98, 152, 196, 490 nm) were measured by ellipsometry [28], as shown in Fig. 1b).

The frequency-domain photoreflectance microscopy is one of the most convenient photothermal techniques to measure the thermal diffusivity of solid materials. It uses an intensity-modulated green laser (λ = 532 nm) focused by an optical microscope onto the surface of the sample [21,29]. The modulated beam excites thermal "waves", and the resulting distribution of the surface temperature modulation is read by a second probe laser (λ = 670 nm) using the temperature dependence of the reflectivity, which is proportional to temperature in a first approximation, and depends on the nature of the reflecting material. The amplitude and the phase of the modulated photoreflectance signals are extracted by lock-in detection and recorded as a function of the distance between the two spots. This method requires a good absorption of the heating laser, for efficient thermal wave generation, and an efficient reflection of the probe laser. In the case of transparent materials, an opaque and reflective transducing surface is therefore always needed in order to create and probe the thermal waves. In our case, the Al_2O_3 and SiO_2 samples were coated with a 100 nm thick gold layer. The measurements were performed at room temperature, with an excitation frequency of 150 kHz. The heat diffusion theoretical model depends on an effective diameter, which is obtained by a convolution of the heating laser spot and the probing laser spot. This effective diameter was found to be 3 μm, a value which can be either determined by convolution of the Airy discs associated to the laser wavelengths and the numerical aperture of the objective, or by fitting measurements obtained on a known sample.

3. Results and discussion

The thermal diffusivity D of an optically and thermally thick, isotropic, bulk material can be straightforwardly extracted from the slope $\frac{dP}{dx} = \sqrt{\frac{\pi f}{D}}$ of the phase lag P of the surface temperature rise with respect to the excitation at a distance x from the excitation, where f is the excitation frequency [30]. For a multilayered sample, there is no such simple relation, since the phase slope.

$\frac{dP}{dx}$ is then a function of the diffusivities and conductivities of the different layers [29]. However, the surface temperature modulation can be calculated using a thermal quadrupole formalism [25]. The thermal diffusivity and conductivity of one layer of known thickness is therefore obtained by using this model and determining the thermal properties which best fit the measured amplitude and phase of the surface temperature modulation. The samples are considered homogenous laterally over the studied region (40 μm), and the anisotropy of the diffusion coefficient, i.e. differences between the in-plane and through-plane diffusion coefficients, $D_{//}$ and $D_{\perp}$ respectively, are neglected. Moreover, the diffusivity and conductivity are not determined independently, but rather upon assuming that the ratio of thermal conductivity k to thermal diffusivity D is constant $\frac{k}{D} = \rho C$=cst, with ρ the density and C the specific heat of the bulk material, taken from the literature. In some cases, e.g. when the thermal contrast and the measurement Signal to Noise Ratio are sufficient, the thermal parameters of up to two media [29] can be obtained simultaneously. However, because the number of variables increases with each additional layer, a reliable determination of the thermal properties of a given layer requires the precise knowledge of the thicknesses and thermal properties of the other layers. Therefore, the thermal properties of the different layers composing the samples were determined in three steps, depicted in Fig. 2:

- Step 1: A gold layer was deposited simultaneously on glass and on the studied samples. Since its thermal properties are well known, and because it is thermally insulating, glass is an appropriate choice to study the properties of the 100 nm gold layer which essentially drive the surface temperature.
- Step 2: An identical gold layer was deposited on a bare Si substrate, to characterize the thermal properties of the substrate.
- Step 3: An identical substrate, supporting the layers to be characterized and the same gold layers was fabricated. Using the properties obtained in steps 1 and 2, the thermal properties of the relevant layer can finally be measured.

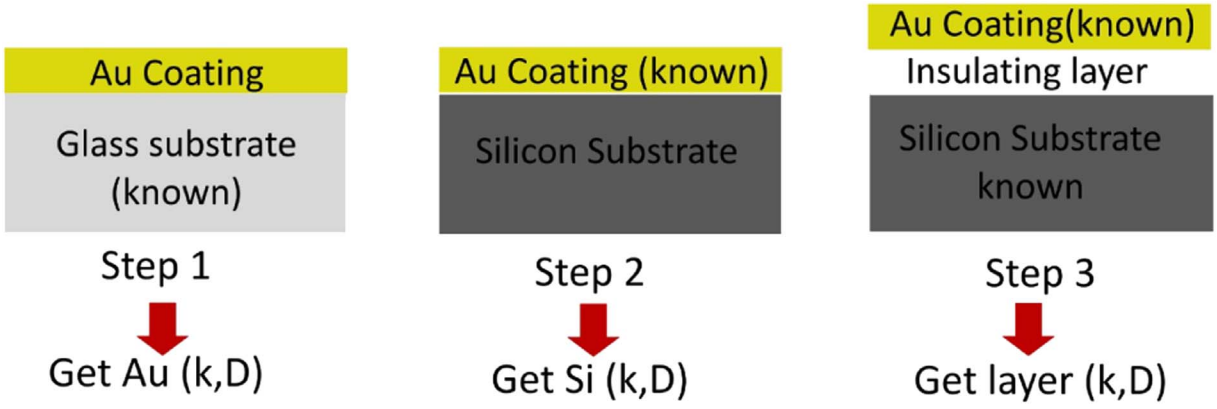

Fig. 2. Schematic of the analysis procedure.

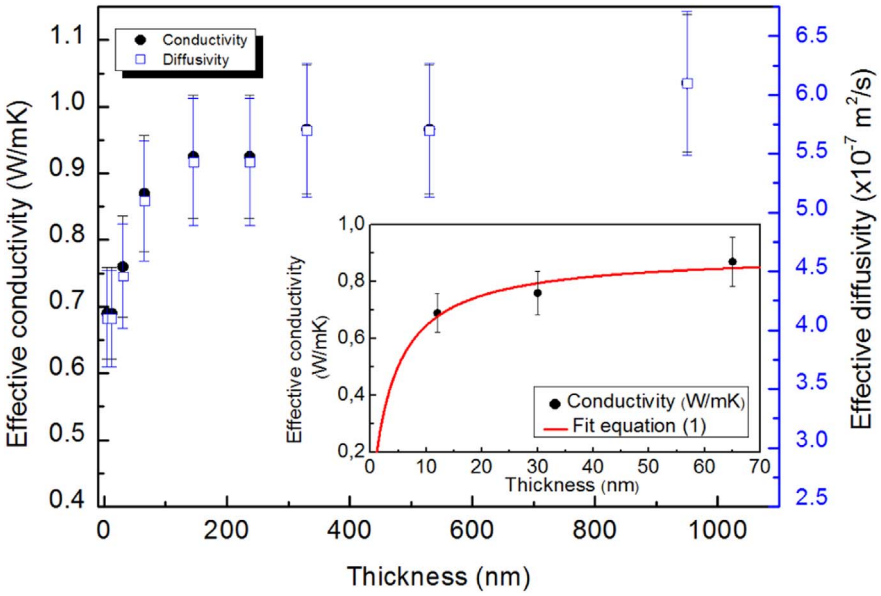

Fig. 3. Effective thermal conductivity and diffusivity versus thickness of SiO_2 layer over doped Si substrate. The symbols are the measured values along with the corresponding uncertainties. The inset solid line corresponds to the best fit following Eq. (1); the obtained parameters are $k_i = 0.95$ W/m·K and $R_{th} = 5.1 \times 10^{-9}$ m^{2}K/W.

In two separate runs, using different adhesion layers and under different conditions, gold was deposited on SiO_2 and Al_2O_3 thin films along with a glass reference sample for each run. On top of the SiO_2 layer, we measured a thermal diffusivity $D = 9.6 \times 10^{-5}$ m^2/s and a thermal conductivity k = 238 W/m·K for the gold layer. The density of gold and its specific heat were taken from literature [31]: 19.3×10^3 kg/m^3 and 128 J/kg·K respectively. On top of the Al_2O_3 layers, the measured thermal diffusivity and conductivity of gold were found to be $D = 6.2 \times 10^{-5}$ m^2/s and k = 155 W/m·K respectively. The same gold is deposited simultaneously over all samples of the same kind; thus it is reasonably assumed that the gold coating measured in step 1 has identical properties over the same series.

Similarly, a precise substrate characterization was then obtained by taking measurements on substrates coated simultaneously with the same gold film (step 2). The substrate for both series is silicon, and the ratio $\frac{k}{D} = \rho C$ was kept constant [32] at 16.7×10^5 J/m^{3}K, following the Dulong-Petit law. The substrate used for all the SiO_2 samples is a p-type (boron) doped silicon with 0.001–0.01 Ohm.cm resistivity. Its thermal properties were found to be $D = 4.5 \times 10^{-5}$ m^2/s and k = 75 W/m·K. The substrate for the Al_2O_3 films, as described above, was not vertically homogeneous since the silicon wafers comprise an epilayer of 10–14 μm n-doped Si. However, at our excitation frequency f = 150 kHz, the penetration depth of thermal waves is given by $\mu = \sqrt{\frac{D}{\pi f}} = 13$ μm. Therefore, thermal waves do not significantly penetrate the underlying undoped silicon, and this substrate can be safely considered as homogeneous, semi-infinite, n-doped silicon. The obtained substrate thermal properties are $D = 8 \times 10^{-5}$ m^2/s and k = 135 W/m·K. Finally (step 3), the properties of each material was determined using the parameters of the appropriate gold coating and substrate obtained in step 1 and 2.

Let us consider SiO_2, a well-studied material, in order to allow comparison with existing measurements. The reported values of micrometric thick films thermal conductivity essentially depend on the deposition technique, and range from 1 to 1.4 W/m·K for SiO_2 grown by thermal oxidation [33–35]. Fig. 3 shows the obtained values of the effective thermal conductivity as a function of thickness. Typical examples of the measurements and theoretical fits quality are shown in the next section. As we scale down thickness (< 100 nm), thin films can be modeled as thermal resistances. In other words, the theoretical fit is mainly affected by the value of $l \cdot k^{-1}$, where l is the thickness. In this case, the change in the thermal properties only affects the amplitude and not the phase, which is dictated by the diffusivity. The inset in Fig. 3 shows the fit of the thermal conductivities of these thin layers as a function of thickness l, by a resistance model [36]:

$$l \cdot k^{-1} = l \cdot k_i^{-1} + R_{th} \quad (1)$$

where $l \cdot k^{-1}$ is the total thermal resistance, R_{th} is the additional interfacial thermal resistance (metal/film and film/substrate interfaces), k_i is the intrinsic thermal conductivity which stands for the upper limit of the effective thermal conductivity reached for the thickest layers. The

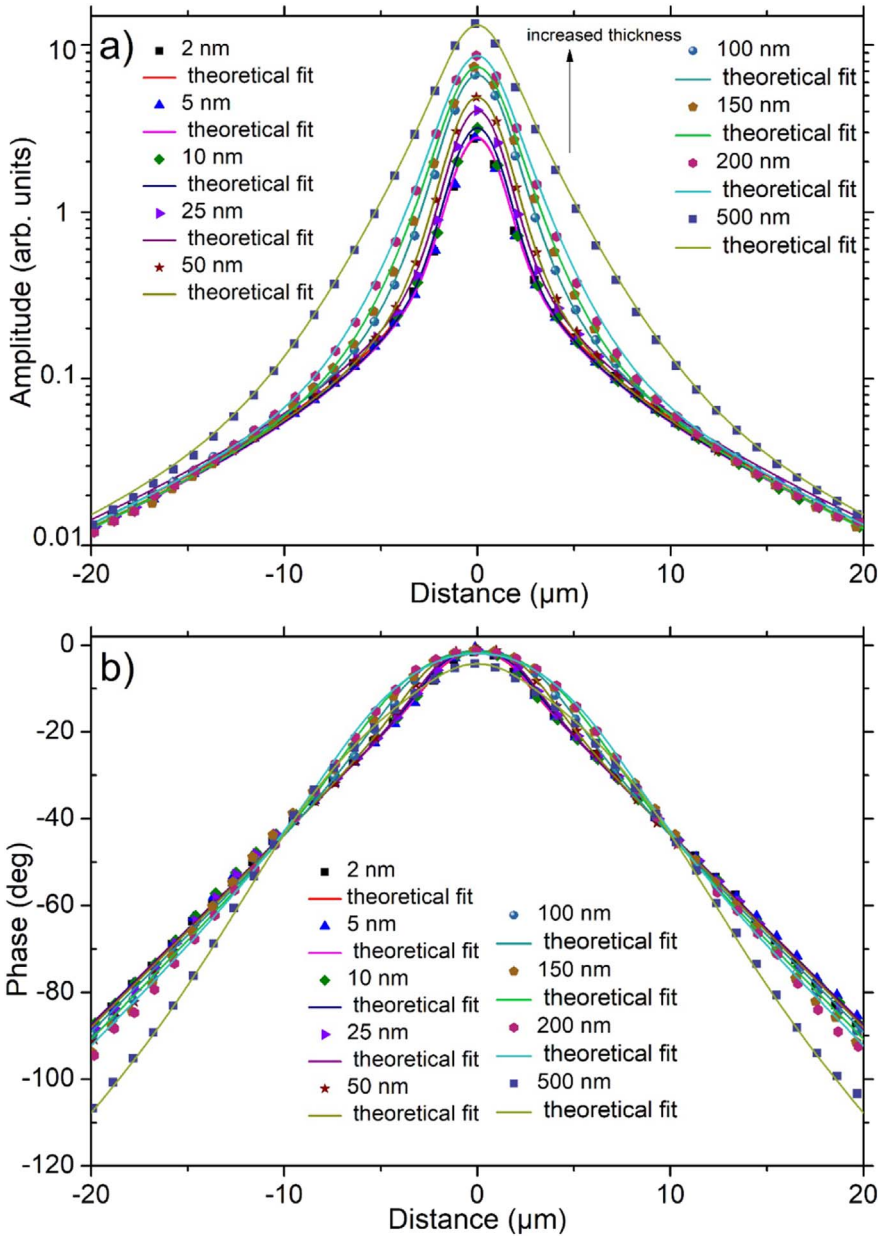

Fig. 4. a) Amplitude and, b) phase of the measured photoreflectance signals along with corresponding fits for different thicknesses of Al_2O_3. The experimental error on the measurement is 5%, and was estimated by repeating each measurement 5 times.

best fit corresponds to an intrinsic thermal conductivity of (0.95 ± 0.03) W/m·K, a value identical (within 5%) to the one reported by Govorkov et al. [33]. We noticed higher discrepancies (30%) compared to values reported by the 3ω method [34] and some similar techniques [35]. These discrepancies could be related to the heat generation/collection method. Photoreflectance excites a sub-μm circular region and probes laterally, whereas resistors used to excite and probe in the 3ω method are usually tens of micrometers wide. While both methods probe a combination of in-plane and through-plane thermal properties, photoreflectance is comparatively more sensitive to in-plane thermal properties, and the 3ω method to through-plane properties. Moreover, it is important to point out that even for the thickest layer, 1 μm, the value of bulk fused silica (1.38 W/m·K) [37] may not be attained. Since thermal transport across multilayer systems is influenced by the thermal boundary resistance, it is important to extract this quantity. In the current study, we deduce the influence of the two interfaces through the best fit of the resistance model (Eq. 1). This resistance was found to be $(5.1 \pm 1) \times 10^{-9}$ m^{2}K/W, approximately 7 times smaller than the values reported by Chien et al. [35]. The uncertainties on k_i and R_{th} are the standard deviation errors on the fitting parameters. For the thicker layers (> 100 nm), the penetration depth, which is in this case equal to 1.3 μm, becomes comparable to the layer thickness; in this range, the thermal resistance model does not hold.

Fig. 4 shows the results obtained over 9 samples with different Al_2O_3 layer thicknesses. Fig. 4a) represents the amplitudes (log scale) and Fig. 4b) the phases of the photoreflectance signals versus the distance from the heating point. The symbols are the experimental results, and solid lines are the corresponding best fits. As can be noticed, each layer thickness yields a measurement which can be clearly distinguished, owing to the fact that Al_2O_3, like SiO_2, is a very insulating material, strongly contrasting with the silicon substrate and gold layer. Each of these measurements is accurately fitted using the parameters measured for the substrate and the gold coating, with the thermal properties of Al_2O_3 as the only variable parameters. In order to avoid any rough assumptions on the native oxide layer (approx. 1.5 nm) found on the Si substrate and the possible presence of a thermal boundary resistance, we used a single equivalent layer with an effective

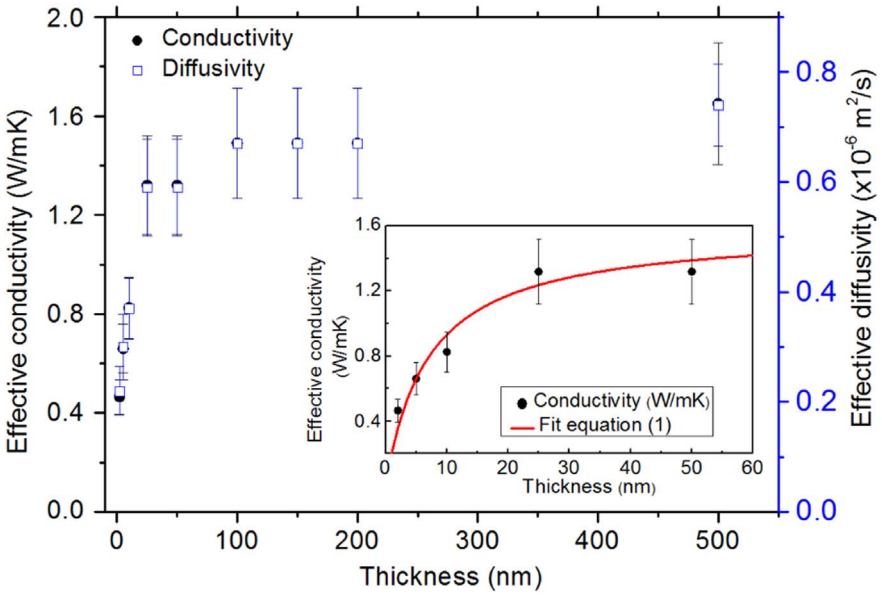

Fig. 5. Effective thermal conductivity and diffusivity versus thickness of Al_2O_3 layer over Si substrate. The symbols are the measured values along with the corresponding uncertainties. The inset solid line corresponds to the best fit following Eq. (1); the obtained parameters are k_i = 1.56 W/m·K and $R_{th} = 4.26 \times 10^{-9}$ m^{2}K/W.

thermal conductivity to describe the oxide and the resistance. The values of Al_2O_3 effective thermal conductivity and thermal diffusivity used to fit the measurements are shown in Fig. 5 as a function of the layer thickness. The ratio $\frac{k}{D} = \rho C = 2.2 \times 10^6$ J/m^{3}K was kept constant upon fitting all the measurements, with ρ the density of amorphous Al_2O_3 and C the specific heat taken from literature [16] to be 2.95×10^3 kg/m^3 and 755 J/K·kg, respectively. The precision on the reported values of thermal conductivity and diffusivity is presented in Fig. 5 by error bars. The error bars were determined by varying the fitting parameters until all measurement points, both in amplitude and in phase, were comprised between curves corresponding to D ± ΔD or k ± Δk. These values of ΔD or Δk were then adopted as measurement uncertainties. The values of the effective thermal conductivity were found to vary between 1.65 and 0.465 W/m·K, and those of the diffusivity between $(0.74 \text{ and } 0.22) \times 10^{-6}$ m^2/s depending on the thickness. One can note a strong drop in the thermal conductivity of Al_2O_3 below 20 nm, which could possibly be caused by mechanical stress in the first few atomic layers. Indeed, optical refractive index measurements in sub-50 nm films [38] have shown that annealing, which precisely relieves this stress, has a strong influence on these properties, and could similarly impact the thermal properties. However, between 98 nm and 2 nm layer thickness, Al_2O_3 films behave as thermal resistances, and we used the model expressed in Eq. (1), as shown in the inset in Fig. 5. Note that we retrieve a value for the intrinsic thermal conductivity of k_i = (1.56 ± 0.08) W/m·K, which is close to the value of effective thermal conductivity of the thickest layer. The thermal resistance was found to be equal to $(4.26 \pm 0.67) \times 10^{-9}$ m^{2}K/W, which corresponds to the effective resistance of the two interfaces. Let us remark that the analysis of the experimental data based on Fourier's heat equation seems to stay reasonable despite the few-nanometers thicknesses involved. We could not identify clearly a further reduction of the thermal conductivity, as would be the case if ballistic transport were happening, for the smallest thicknesses within our experimental accuracy. This could be due to the fact that diffusion still holds at such scale for amorphous, i.e. disordered, media.

4. Conclusion

In summary, we presented a study of the thermal properties of SiO_2 and Al_2O_3 thin films as a function of thickness. For low thicknesses, 12 nm for SiO_2 and 2–5 nm for Al_2O_3, we measured reductions of the effective thermal conductivity by 30% and 70% compared to the values obtained for micrometric layers of SiO_2 and Al_2O_3 respectively. The interfacial thermal resistance was small in both cases, suggesting good thermal transport across the interfaces. The diffusivity and conductivity are not measured independently, but rather upon the assumption that ρC = cst, though the effect of diffusivity is clearly revealed by the change of the phase of the photoreflectance signal for the thick layers (down to 100 nm). The thermal conductivity and diffusivity were determined with an average precision of 15%, except for the 10, 5 and 2 nm thick layers of Al_2O_3. For these very thin films, the precision is 20%, although the absolute value of the uncertainty is unchanged. The different recorded response for each measured layer proves that frequency domain photoreflectance microscopy is a well-adapted robust technique to analyze thin films down to the nanometric scale.

Acknowledgments

This work was funded by the European Union Seventh Framework Program FP7-NMP-2013-LARGE-7 under grant agreement number 8604668 “Quantiheat”. The authors would like to thank L. Aigouy and L Billot for the gold coatings deposition.

References

[1] G. Zhu, H. Lee, Y. Lan, X. Wang, G. Joshi, D. Wang, J. Yang, D. Vashaee, H. Guilbert, A. Pillitteri, et al., Increased phonon scattering by nanograins and point defects in nanostructured silicon with a low concentration of germanium, Phys. Rev. Lett. 102 (19) (2009) 196803.
[2] X. Wang, H. Lee, Y. Lan, G. Zhu, G. Joshi, D. Wang, J. Yang, A. Muto, M. Tang, J. Klatsky, et al., Enhanced thermoelectric figure of merit in nanostructured n-type silicon germanium bulk alloy, Appl. Phys. Lett. 93 (19) (2008) 193121.
[3] G. Chen, P. Hui, Thermal conductivities of evaporated gold films on silicon and glass, Appl. Phys. Lett. 74 (20) (1999) 2942–2944.
[4] G. Langer, J. Hartmann, M. Reichling, Thermal conductivity of thin metallic films measured by photothermal profile analysis, Rev. Sci. Instrum. 68 (3) (1997) 1510–1513.
[5] M. Kazan, S. Volz, Calculation of the lattice thermal conductivity in granular crystals, J. Appl. Phys. 115 (7) (2014) 073509.
[6] B. Gotsmann, M. Lantz, Quantized thermal transport across contacts of rough surfaces, Nat. Mater. 12 (1) (2013) 59–65.
[7] L. Jalabert, T. Sato, T. Ishida, H. Fujita, Y. Chalopin, S. Volz, Ballistic thermal conductance of a lab-in-a-tem made Si nanojunction, Nano Lett. 12 (10) (2012) 5213–5217.
[8] I. Stark, M. Stordeur, F. Syrowatka, Thermal conductivity of thin amorphous alumina films, Thin Solid Films 226 (1) (1993) 185–190.
[9] S.-M. Lee, D.G. Cahill, T.H. Allen, Thermal conductivity of sputtered oxide films, Phys. Rev. B 52 (1) (1995) 253.
[10] A. Cai, L.-p. Yang, J.-p. Chen, T.-g. Xi, S.-g. Xin, W. Wu, Thermal conductivity of anodic alumina film at (220 to 480) K by laser flash technique, J. Chem. Eng. Data 55 (11) (2010) 4840–4843.
[11] A. Cappella, J.-L. Battaglia, V. Schick, A. Kusiak, A. Lamperti, C. Wiemer, B. Hay,

High temperature thermal conductivity of amorphous Al_2O_3 thin films grown by low temperature ALD, Adv. Eng. Mater. 15 (11) (2013) 1046–1050.
[12] Patrick E. Hopkins, Thermal transport across solid interfaces with nanoscale imperfections: effects of roughness, disorder, dislocations, and bonding on thermal boundary conductance, ISRN Mechanical Engineering 2013, 2013.
[13] G. Dingemans, W. Kessels, Status and prospects of Al_2O_3-based surface passivation schemes for silicon solar cells, J. Vac. Sci. Technol. A 30 (4) (2012) 040802.
[14] E. Langereis, M. Creatore, S. Heil, M. Van de Sanden, W. Kessels, Plasma-assisted atomic layer deposition of Al_2O_3 moisture permeation barriers on polymers, Appl. Phys. Lett. 89 (8) (2006) 081915.
[15] S. Potts, W. Keuning, E. Langereis, G. Dingemans, M. Van de Sanden, W. Kessels, Low temperature plasma-enhanced atomic layer deposition of metal oxide thin films, J. Electrochem. Soc. 157 (7) (2010) P66–P74.
[16] M. Groner, F. Fabreguette, J. Elam, S. George, Low-temperature Al_2O_3 atomic layer deposition, Chem. Mater. 16 (4) (2004) 639–645.
[17] S. Ferrari, F. Perissinotti, E. Peron, L. Fumagalli, D. Natali, M. Sampietro, Atomic layer deposited Al_2O_3 as a capping layer for polymer based transistors, Org. Electron. 8 (4) (2007) 407–414.
[18] S.E. Gustafsson, Transient plane source techniques for thermal conductivity and thermal diffusivity measurements of solid materials, Rev. Sci. Instrum. 62 (3) (1991) 797–804.
[19] D.G. Cahill, Heat transport in dielectric thin films and at solid-solid interfaces, Microscale Thermophys. Eng. 1 (2) (1997) 85–109.
[20] A. Rosencwaig, J. Opsal, W. Smith, D. Willenborg, Detection of thermal waves through optical reflectance, Appl. Phys. Lett. 46 (11) (1985) 1013–1015.
[21] L. Pottier, Micrometer scale visualization of thermal waves by photoreflectance microscopy, Appl. Phys. Lett. 64 (13) (1994) 1618–1619.
[22] L. Fabbri, D. Fournier, L. Pottier, L. Esposito, Analysis of local heat transfer properties of tape-cast AlN ceramics using photothermal reflectance microscopy, J. Mater. Sci. 31 (20) (1996) 5429–5436.
[23] B. Li, L. Pottier, J. Roger, D. Fournier, K. Watari, K. Hirao, Measuring the anisotropic thermal diffusivity of silicon nitride grains by thermoreflectance microscopy, J. Eur. Ceram. Soc. 19 (8) (1999) 1631–1639.
[24] C. Frétigny, J.P. Roger, V. Reita, D. Fournier, Analytical inversion of photothermal measurements: independent determination of the thermal conductivity and diffusivity of a conductive layer deposited on an insulating substrate, J. Appl. Phys. 102 (11) (2007) 116104.
[25] K. Plamann, D. Fournier, B.C. Forget, A.C. Boccara, Microscopic measurements of the local heat conduction in polycrystalline diamond fillms, Diam. Relat. Mater. 5 (6) (1996) 699–705.
[26] Parameswaran Hariharan, Basics of Interferometry, Academic Press, 2010.
[27] M. Ville, et al., Crystallinity of inorganic films grown by atomic layer deposition: overview and general trends, J. Appl. Phys. 113 (2) (2013) 2.
[28] Hiroyuki Fujiwara, Spectroscopic Ellipsometry: Principles and Applications, John Wiley & Sons, 2007.
[29] B. Li, J. Roger, L. Pottier, D. Fournier, Complete thermal characterization of film-on-substrate system by modulated thermoreflectance microscopy and multiparameter fitting, J. Appl. Phys. 86 (1999) 5314–5316.
[30] A. Salazar, A. Sanchez-Lavega, Thermal diffusivity measurements using linear relations from photothermal wave experiments, Rev. Sci. Instrum. 65 (9) (1994) 2896–2900.
[31] G.W.C. Kaye, Laby, Tables of Physical and Chemical Constants, Longmans, Green and Company, 2008 Version 1.1.
[32] M.S. Shur, Handbook Series on Semiconductor Parameters, vol. 1, World Scientific, 1996.
[33] S. Govorkov, W. Ruderman, M. Horn, R. Goodman, M. Rothschild, A new method for measuring thermal conductivity of thin films, Rev. Sci. Instrum. 68 (10) (1997) 3828–3834.
[34] T. Yamane, N. Nagai, S.I. Katayama, M. Todoki, Measurement of thermal conductivity of silicon dioxide thin films using a 3omega method, J. Appl. Phys. 91 (2002) 9772–9776.
[35] H.C. Chien, D.J. Yao, M.J. Huang, T.Y. Chang, Thermal conductivity measurement and interface thermal resistance estimation using SiO_2 thin film, Rev. Sci. Instrum. 79 (5) (2008) 054902.
[36] B. Belkerk, S. Bensalem, A. Soussou, M. Carette, H. Al Brithen, M. Djouadi, Y. Scudeller, Substrate-dependent thermal conductivity of aluminum nitride thin-films processed at low temperature, Appl. Phys. Lett. 105 (22) (2014) 221905.
[37] Y.S. Touloukian, C. Ho, Thermal conductivity. nonmetallic solids, Thermophysical properties of matter-The TPRC Data Series, IFI/Plenum, New York, 1970.
[38] Z.Y. Wang, et al., The impact of thickness and thermal annealing on refractive index for aluminum oxide thin films deposited by atomic layer deposition, Nanoscale Res. Lett. 10 (1) (2015) 46.